Monthly Notices
of the
ROYAL ASTRONOMICAL SOCIETY

MNRAS **494,** 3536–3540 (2020) doi:10.1093/mnras/staa841

Progress of liquid crystal adaptive optics for applications in ground-based telescopes

Xingyun Zhang [1], Zhaoliang Cao,[2] Quanquan Mu,[1,3]★ Dayu Li,[1] Zenghui Peng,[1] Chengliang Yang,[1] Yonggang Liu[1] and Li Xuan[1]

[1]*State Key Laboratory of Applied Optics, Changchun Institute of Optics, Fine Mechanics, and Physics, Chinese Academy of Sciences, Changchun, Jilin 130033 China*
[2]*School of Mathematics and Physics, Suzhou University of Science and Technology, Suzhou, Jiangsu 215009, China*
[3]*Center of Materials Science and Optoelectronics Engineering, University of Chinese Academy of Sciences, Beijing 100049, China*

Accepted 2020 March 23. Received 2020 March 23; in original form 2019 September 10

ABSTRACT

Liquid crystal (LC) adaptive optics systems (AOS) can potentially be used in ground-based large aperture telescopes, because of their high spatial resolution, low cost and compact size. However, their disadvantages, such as low energy efficiency and slow response speed, still hinder their application. In this paper, we demonstrate solutions to these problems. With newly synthesized fast nematic LC material and using an overdriving technique, the response time of a LC wavefront corrector was reduced to 0.75 ms. Under an open-loop control scheme, a novel optical system was designed to improve the energy efficiency of LC AOS. With those problems resolved, a LC AOS was built for a 1.23-m telescope. This system has a disturbance rejection bandwidth of 80 Hz, and could fully use the energy of 400–900 nm wavebands. Observation results showed that the diffraction limit resolution imaging of the telescope could be obtained after correction, which indicates that the LC AOS is ready to be used in ground-based telescopes for visible waveband imaging.

Key words: instrumentation: adaptive optics – techniques: miscellaneous.

1 INTRODUCTION

Even though adaptive optics (AO) have been used in ground-based large-aperture telescopes to improve their imaging resolution for over 30 yr, up to now most AO systems (AOS) still work in near infrared rather than the visible range. Visible AO have higher resolution with darker skies (Close 2016), but require many more actuators for the wavefront corrector, which is normally a deformable mirror. Up to now, the most advanced deformable mirror is used in PALM-3000 with 3388 actuators (Roberts et al. 2012). This is far from the requirement of visible AO for extremely large telescopes such as the Thirty Meter Telescope (TMT) and the Extremely Large Telescope (ELT).

A liquid crystal (LC) wavefront corrector (WFC), made using nematic LC, may match this demand. Because nematic LC is widely used in liquid crystal displays (LCDs), and is convenient to realize phase modulation because of its birefringence property, LCWFCs could have high spatial resolution (i.e. millions of pixels), compact size and low cost. Hence, the use of LCWFCs in visible AO for ground-based large-aperture telescopes is very promising. However, LCWFCs still have the disadvantages of slow response speed and low energy efficiency. The response time of nematic LC material is normally longer than 10 ms. Hattori & Komatsu (2002) proposed a LC adaptive optics system (AOS) based on a nematic LCWFC, which has a response time of 30 ms; for AO applications in ground-based telescopes, the response time should be reduced to less than 1 ms at least. The response time of dual-frequency LC (Gu et al. 2004) and ferroelectric LC (Burns et al. 1995) could match this demand. However, the high driving voltage requirement of dual-frequency LC and the binary phase modulation of ferroelectric LC limit their performance.

The energy efficiency of LCWFCs is low because it is polarization-dependent and only works in a narrow waveband. Love (1993) and Love et al. (1996) proposed several methods to avoid polarization dependence, but these methods either decrease the response speed of the LCWFC or lead to fabrication difficulties. To extend the working waveband, Stockley et al. (1995) utilized chiral smectic ferroelectric LC to obtain a non-dispersive LCWFC, but this has a low quantified phase level and amplitude modulation.

So the hope of applying LC AOS in ground-based telescopes still relies on nematic LCWFCs. So far, nematic LCWFCs are still mainly used in AOS for applications such as retina imaging systems (Shirai et al. 2009; Kong et al. 2012) or fluorescence microscopy (Wang et al. 2014; Liu et al. 2018), where the light source (laser

★ E-mail: muquanquan@ciomp.ac.cn

or fluorescence) is monochromatic and the wavefront aberration changes slowly (e.g. in biological tissue).

Our working group has studied LC AOS (based on nematic LCWFCs) for more than 10 yr. Unlike others, we utilized novel optical design to improve the energy efficiency of LC AOS (Mu et al. 2010; Cao et al. 2012). Fast-response nematic LC material is designed and synthetized (Peng et al. 2013), and an overdriving technique (Nakamura, Crain & Sekiya 2001) is adopted to further increase the response speed of LCWFCs (Hu et al. 2012).

Up to now, the energy efficiency and system bandwidth of LC AOS have been improved drastically, and the performance is compatible with AOS based on deformable mirrors. So, we built a LC AOS for a 1.23-m telescope, located at Changchun Institute of Optics, Fine Mechanics and Physics (CIOMP). Observations have shown that diffraction limit resolution imaging of the telescope could be obtained for a star, and a binary system with the angular separation of 0.2 arcsec could be resolved clearly after correction. All results indicate that, after decades of research, LC AOS can now be used in large-aperture telescopes for visible waveband imaging.

2 FAST RESPONSE LCWFCS

Fast-response LCWFCs are the key factor to improve the system bandwidth of LC AOS. Fast-response nematic LC material and an overdriving technique are investigated to increase the response speed of LCWFC.

2.1 Fast-response liquid crystal material

Gauza et al. (2003) defined a figure-of-merit (FoM) value to describe the response performance of LC material as

$$FoM = K_{11}{\gamma_1}^{-1}\Delta n^2, \quad (1)$$

where $K_{11}{\gamma_1}^{-1}$ is the visco-elastic coefficient and Δn is the birefringence of LC. The LC with higher Δn and lower viscosity will have a higher *FoM* value and faster response.

The LC group with benzene isothiocyanate always has high birefringence and relatively low viscosity; see Gauza et al. (2005) who designed a high Δn (0.33 at $\lambda = 785$ nm and 35 °C) LC mixture (SG2), with a *FoM* of 13.9 $\mu m^2\ s^{-1}$. This is remarkable as the Δn of the LC used in the LCD industry is around 0.1.

To further enhance the response performance of LC, we synthesized fluorinated phenyl-tolane isothiocyanate LC compounds with chemical structures, as shown in Fig. 1. The highly conjugated molecular structure improves the Δn value to about 0.5 (Peng et al. 2016). Simultaneously, the multi-fluorine substitution reduces the viscosity. With these LC compounds dissolved in the SG2 LC mixture, the Δn of the LC mixture could be improved to 0.42 (at $\lambda = 785$ nm and 40 °C), and the *FoM* could be improved to 41.5 $\mu m^2\ s^{-1}$, which is three times that synthesized by Gauza et al. (2005). With the cell gap optimally designed (Peng et al. 2011), the response time of the LC mixture mentioned above is measured, as shown in Fig. 2. The full phase modulation is 1.35 λ ($\lambda = 785$ nm), and the response time is about 3 ms at 45 °C, which is ten times faster than the LC material used by Hattori & Komatsu (2002).

2.2 Overdriving technique

As shown in Fig. 2, the response of LC is exponential and moves very slowly at the end. The response of the first stage is actually fast; it only takes 0.75 ms to reach the 1 λ cut-off point of the phase modulation. Based on the phase wrapping technique (Jordan et al. 1970; Xuan et al. 2012), 1 λ phase modulation is sufficient for a LCWFC to generate a large correction depth (Liu et al. 2006) without any loss of spatial resolution (Mu et al. 2008). However, if we realize 1 λ phase modulation with the conventional driving method, the response time would still be much longer than 0.75 ms, because of the slow response of the last stage.

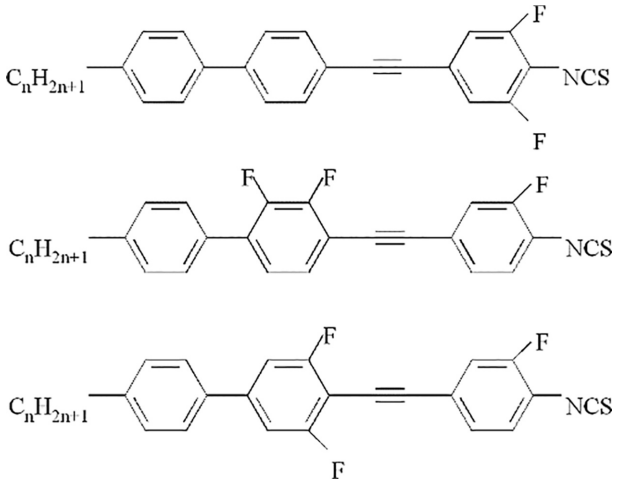

Figure 1. Chemical structures of synthesized LC compounds.

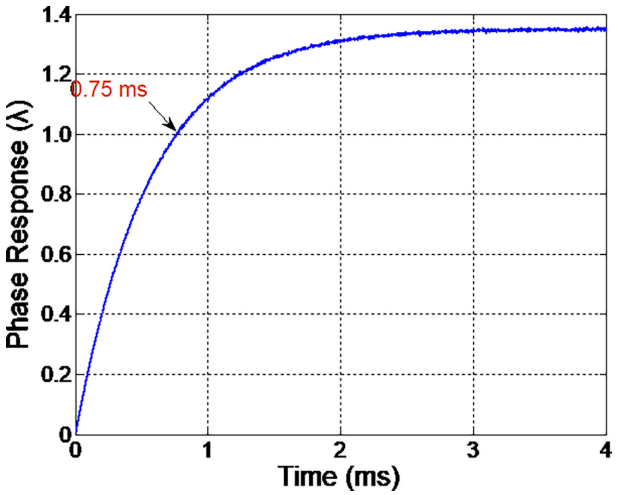

Figure 2. Phase modulation of the synthesized LC mixture as a function of time ($\lambda = 785$ nm).

To solve this problem, we adopt an overdriving technique, which is commonly used to reduce the response time of LCDs (Nakamura et al. 2001), as shown in Fig. 3. The driving signal of the current phase and the target phase are G_I and G_F, respectively. If we apply the driving signal G_F directly at t_1, the response of the LC would follow the purple dotted curve, and the response time would be $t_3 - t_1$. However, if we apply a transitional driving signal G_T (where $G_I - G_T > G_I - G_F$) at t_1, and then apply G_F when the LC reaches the target phase at t_2, the response of LC would follow the blue solid curve, and the response time would be $t_2 - t_1$ ($< t_3 - t_1$).

With the fast-response LC material described in Section 2.1 and the overdriving technique, we developed the fastest LCWFC in the world, with the help of Meadowlark Corporation (Meadowlark is in charge of the driver part, and the LC material is supplied by us). This LCWFC is a liquid crystal on silicon device with 256 × 256 pixels and 6.14 × 6.14 mm aperture size, and the temperature is

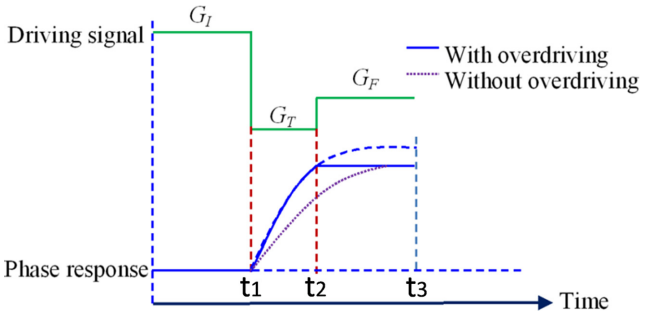

Figure 3. Demonstration of the overdriving technique.

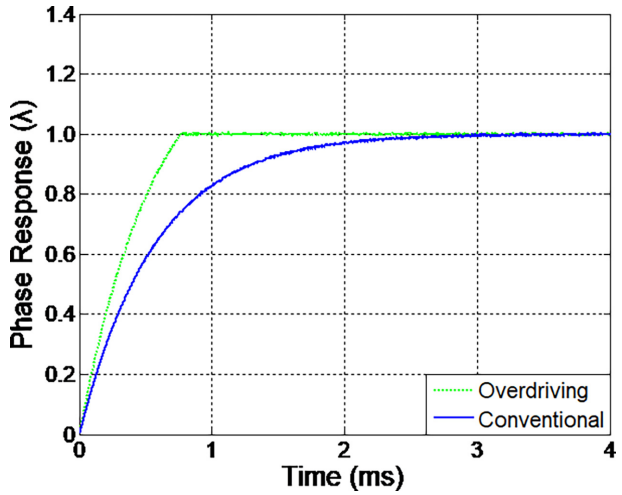

Figure 4. Phase modulation as a function of time without and with the overdriving technique ($\lambda = 785$ nm).

controlled to be around 45 °C. The decay response of the LCWFC was measured when the phase modulation changes from 0 to 1 λ (λ = 785 nm), which is the slowest process of this device, because 1 λ is the maximum modulation required by the phase wrapping technique. The response time without and with the overdriving technique is about 3.0 and 0.75 ms, respectively. The response speed is improved by four times with the overdriving technique (see Figure 4).

3 NOVEL OPTICAL DESIGN

Normally, an AOS works in a closed loop, as shown in Fig. 5, where the sensor (WFS) is located 'behind' the corrector (LCWFC), so that the WFS can measure the correction residual of theLCWFC. The TTM is a tip–tilt mirror, which is used to compensate for the low-order aberrations (tip and tilt). The BPF is a bandpass (700–900 nm) filter, which will cause a lot of energy loss but it is indispensable, as the LCWFC only works in a narrow waveband. The LCWFC is also polarization-dependent, so a polarizer (P) is needed, which will cause another 50 per cent energy loss. Under such set-up, only 50 per cent of the energy of the 700–900 nm wavebands is usable. Furthermore, the 50 per cent energy of the 700–900 nm wavebands must be divided into two parts: 25 per cent into a wavefront sensor (WFS) for wavefront detection, and 25 per cent into a CCD for imaging. This type of energy efficiency is not acceptable for astronomical observations.

In order to improve the energy efficiency of the LC AOS, we designed an optimal optical set-up based on an open-loop control

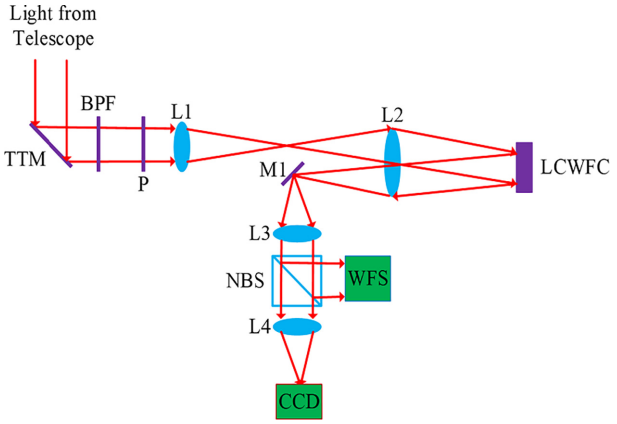

Figure 5. Schematic diagram of a closed-loop LC AOS.

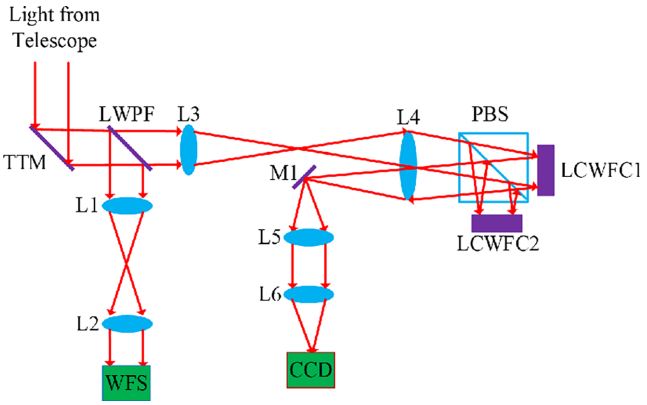

Figure 6. Schematic diagram of an open-loop LC AOS.

scheme, as shown in Fig. 6. The light coming from the object is split into two beams by a long-wave pass filter (LWPF): the reflected beam with the waveband of 400–700 nm goes to the WFS for wavefront detection, and the transmitted beam with the 700–900 nm waveband is split into two linear polarized beams with a polarized beam splitter (PBS) and corrected by two LCWFCs. Finally, the corrected beams are combined and imaged with a CCD. Based on this optical set-up, the LC AOS could fully use the energy of 400–900 nm wavebands. Different from the closed-loop LC AOS shown in Fig. 5, the WFS is parallel rather than behind the LCWFCs, so the open-loop LC AOS must be controlled by means of feed-forward.

4 RESULTS

4.1 System configuration and performance test

Based on the above improvements, a LC AOS was built for the 1.23-m telescope, as shown in Fig. 7. The light coming from the telescope (yellow line) is reflected by the TTM and split into two beams by the LWPF. The reflected beam with the 400–700 nm waveband is detected by a Shack–Hartmann (S–H) WFS, and the transmitted light with the 700–900 nm waveband is split into two linear polarized beams with the PBS and corrected by two LCWFCs. Then, images are obtained using an EM-CCD camera (DU888, Andor). This camera has 1024 × 1024 pixels, a pixel size of 13 μm, and it works at a frame rate of 26 Hz. The TTM (S-334, PI) has a resonant frequency of 2.3 kHz and an optical diameter of

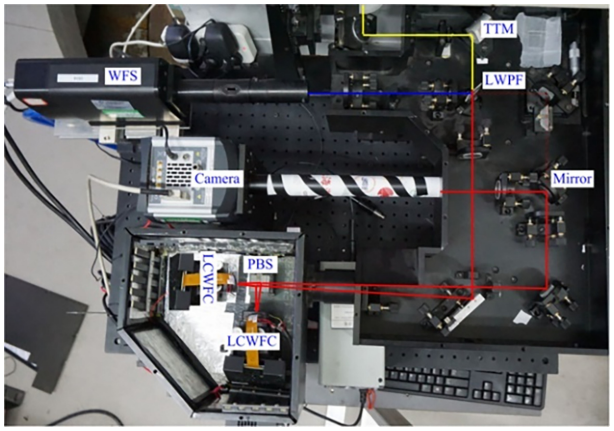

Figure 7. LC AOS configuration for the 1.23-m telescope.

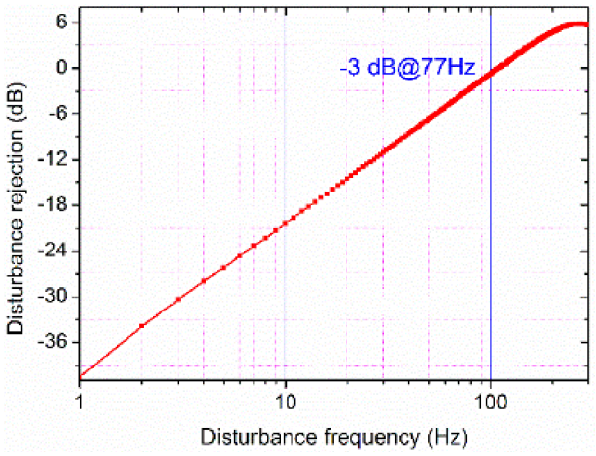

Figure 8. Disturbance rejection ability of the TTM; the –3 dB bandwidth is 77 Hz.

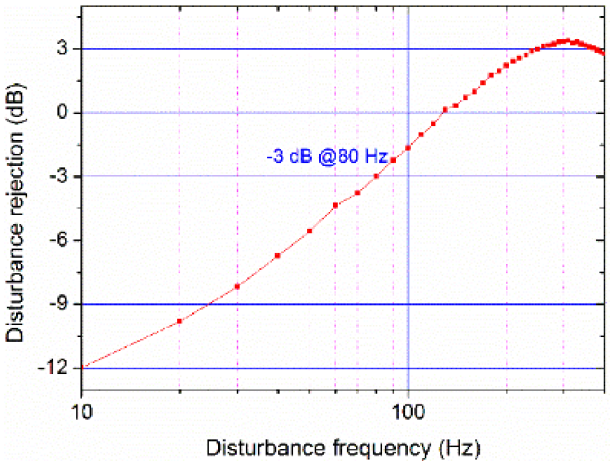

Figure 9. Disturbance rejection ability of the LCWFCs; the –3 dB bandwidth is 80 Hz.

10 mm. The S–H WFS has 15 × 15 micro-lenses and works on an acquisition frequency of 1.33 kHz.

For the designed LC AOS, the TTM works in a closed loop, and the LCWFCs in an open loop. To estimate the correction ability of dynamic aberrations, the system bandwidths for the TTM and LCWFCs were measured with the method proposed by Dayton et al. (2001). Another TTM was introduced into the system, and generated tilt aberrations with different sinusoidal frequencies. The amplitudes of the tilt with and without correction were measured for each frequency. Then the disturbance rejection bandwidth is defined as the frequency at which half the disturbance power is rejected, and this reject point is at –3 dB after calculation with equation (2). The measured rejection bandwidth of low-order aberrations (tip and tilt, corrected by the TTM) is 77 Hz, as shown in Fig. 8. The amplitude of input aberrations was 4.0 waves (at 800 nm).

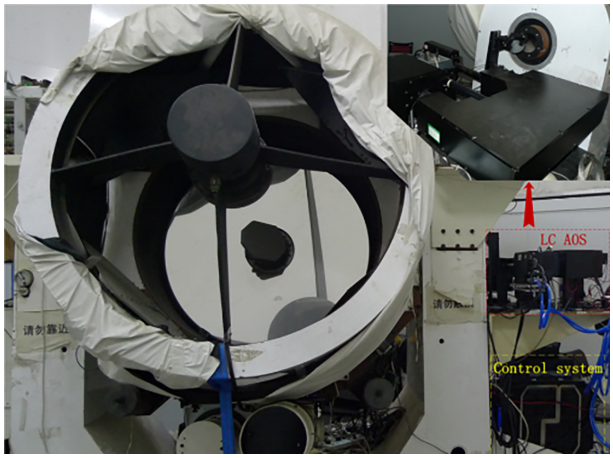

Figure 10. Configuration of 1.23-m telescope with the LC AOS.

$$rej(dB) = 20\log_{10}\left(\frac{Residual}{Disturbance}\right), \quad (2)$$

Furthermore, the disturbance rejection ability of LCWFCs is tested. Because the LCWFCs are controlled in an open loop, the correction residuals cannot be measured by the WFS in Fig. 7. Therefore, in order to measure the rejection bandwidth of LCWFCs, the camera in Fig. 7 is replaced with another WFS. As the rejection of high-order aberrations is difficult to measure, we measured the tilt rejection instead (Dayton et al. 2001). The measured rejection bandwidth is 80 Hz, as shown in Fig. 9. The amplitude of input aberrations was also 4.0 waves (at 800 nm).

4.2 Observation results

The LC AOS was installed on the 1.23-m telescope in 2016 June for long-term testing. The system is placed at the Nasmyth focus of the telescope, and the configuration is shown in Fig. 10. The whole equipment is installed at the forked arm of the telescope; its magnified photograph is shown at the top-right corner, and the bottom-right corner shows the control system of the LC AOS.

After several years of observations, some typical observation results are presented as follows. On 2016 October 28, the star Alpheratz was observed with an apparent magnitude of 2.06 mag. Just before the observation, the atmospheric coherence length was measured to be about 6 cm (at 550 nm wavelength). The images of Alpheratz without and with adaptive correction are shown in Fig. 11, with an exposure time of 1.0 ms and an EM gain of 500. The maximum intensities measured by the CCD without and with correction are 7811 and 32 604 respectively, which is an improvement of about 4.17 times. The blue dotted line is the measured intensity data, and the red solid line is the Gauss fitted curve. To illustrate the change of the full width at half-maximum (FWHM), the measured data without and with correction are normalized. The fitted results show that, without and with correction, the FWHMs are 1.67 and 0.167 arcsec, respectively,

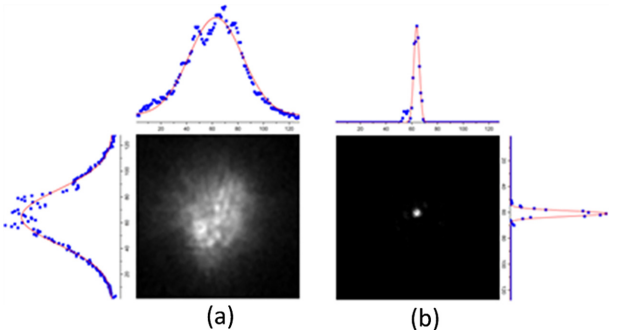

Figure 11. Images of star Alpheratz: (a) without correction; (b) with correction. The dotted line is the measured data, and the solid line is the curve fitted with a Gauss function.

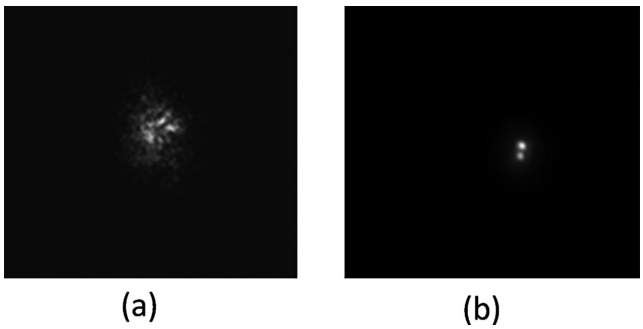

Figure 12. Images of binary system Talitha Australis: (a) before correction; (b) after correction.

at both the *x*- and *y*-axis. The Strehl ratio is improved from 0.1 to 0.96 after correction. As the diffraction limit resolution of the telescope is 0.163 arcsec at the wavelength of 800 nm, we can say that the diffraction limit resolution is obtained with the adaptive correction of the LC AOS.

On 2017 March 18, the binary system Talitha Australis (Kap UMa) was observed, with an angular separation of 0.2 arcsec, and the apparent magnitudes of the two components are 4.16 and 4.54 mag, respectively. The atmospheric coherence length was measured to be about 7 cm (at 550 nm wavelength) just before the observation. As shown in Fig. 12, the binary system could be clearly resolved after the correction of the LC AOS. The exposure time is 3.0 ms and the EM gain is 500 for those images.

5 CONCLUSION

In this paper, we mainly demonstrate the solutions of the shortcomings of LC AOS. First, a fast-response LCWFC is obtained based on fast-response LC material and an overdriving technique. The LCWFC has a response time of 0.75 ms, which is comparable to the performances of deformable mirrors. Therefore, the slow-response problem of the LC AOS is solved.

To solve the low-energy efficiency problem, a novel optical set-up for LC AOS is designed based on open-loop control scheme and waveband splitting method. Wavefront detection uses 400–700 nm wavebands, and the 700–900 nm wavebands is split into two linear polarized beams and then corrected by two LCWFCs. Finally, those two beams are combined into one beam once more for imaging. With this optical set-up, the LC AOS can fully use the energy of 400–900 nm wavebands.

Based on these improvements, a LC AOS is built for the 1.23-m telescope, with –3 dB disturbance rejection bandwidth of about 80 Hz. After AO correction, the diffraction limit resolution imaging of the telescope is obtained for a star, and a binary system with an angular separation of 0.2 arcsec is resolved clearly. All results indicate that after decades of research, the LC AOS is ready to be used in ground-based large-aperture telescopes for visible band imaging.

ACKNOWLEDGEMENTS

This work is funded by the National Natural Science Foundation of China (NSFC) grant nos 61805238, 11774342 and 61475152. The authors are grateful for the support of Professor Qingyun Yang (Photoelectricity Exploration Laboratory, CIOMP) in the operation of the 1.23-m telescope.

REFERENCES

Burns D. C., Underwood I., Gourlay J., O'Hara A., Vass D. G., 1995, Opt. Commun., 119, 623
Cao Z. et al., 2012, Opt. Express, 20, 19331
Close L. M., 2016, Proc. SPIE, 9909, 99091
Dayton D., Browne S., Gonglewski J., Restaino S., 2001, Appl. Opt., 40, 2345
Gauza S., Wang H., Wen C. H., Wu S. T., Seed A. J., Dąbrowski R., 2003, Jpn. J. Appl. Phys., 42, 3463
Gauza S., Li J., Wu S. T., Spadlo A., Dabrowski R., Tzeng Y. N., Cheng K. L., 2005, Liq. Cryst., 32, 1077
Gu D., Winker B., Wen B., Taber D., Brackley A., Wirth A., Albanese M., Landers F., 2004, Proc. SPIE, 5553, 68
Hattori M., Komatsu S., 2002, Opt. Rev., 9, 126
Hu H., Hu L., Peng Z., Mu Q., Zhang X., Liu C., Xuan L., 2012, Opt. Lett., 37, 3324
Jordan J. A., Hirsch P. M., Lesem L. B., Van Rooy D. L., 1970, Appl. Opt., 9, 1883
Kong N., Li C., Xia M., Li D., Qi Y., Xuan L., 2012, J. Biomed. Opt., 17, 026001
Liu T. et al., 2018, Science, 360, 6386
Liu Y., Cao Z., Li D., Mu Q., Hu L., Lu X., Xuan L., 2006, Opt. Eng., 45, 128001
Love G. D., 1993, Appl. Opt., 32, 2222
Love G. D., Restaino S. R., Carreras R. C., Loos G. C., Morrison R. V., Baur T., Kopp G., 1996, OSA summer topical meeting on adaptive optics. Optical Society, Washington DC, p. 288
Mu Q., Cao Z., Li C., Jiang B., Hu L., Xuan L., 2008, Opt. Express, 33, 2898
Mu Q., Cao Z., Hu L., Liu Y., Peng Z., Xuan L., 2010, Opt. Express, 18, 21 687
Nakamura H., Crain J., Sekiya K., 2001, J. Appl. Phys., 90, 2122
Peng Z., Liu Y., Yao L., Cao Z., Mu Q., Hu L., Xuan L., 2011, Opt. Lett., 36, 3608
Peng Z. et al., 2013, Liq. Cryst., 40, 91
Peng Z. et al., 2016, Liq. Cryst., 43, 276
Roberts J. et al., 2012, Proc. SPIE, 8447, 84470Y
Shirai T., Kakeno K., Arimoto H., Furukawa H., 2009, Jpn. J. Appl. Phys., 48, 070213
Stockley J. E., Sharp G. D., Serati S. A., Johnson K. M., 1995, Opt. Lett., 20, 2441
Wang K., MilKie D. E., Saxena A., Engerer P., Misgeld T., Bronner M. E., Mumm J., Betzig E., 2014, Nat. Methods, 11, 625
Xuan L., Cao Z., Mu Q., Hu L., Peng Z., 2012, in Tyson R., ed., Adaptive Optics Progress, Chapter 3. InTech Press, London

This paper has been typeset from a TEX/LATEX file prepared by the author.